

Gravitational Waves from Magnetars

Chris Kouvaris¹

¹*Physics Division, National Technical University of Athens, 15780 Zografou Campus, Athens, Greece*

We study the emission of gravitational waves produced by the magnetosphere of magnetars. We argue that several features in the spectrum could facilitate the identification of that source. In addition, in cases of extremely large magnetic fields we demonstrate that this emission can make the braking index of such stars to be well over 3, which is the standard prediction of the magnetic dipole radiation and aligned rotator mechanisms. A similar picture arises if one focuses on the second braking index. Moreover the braking index depends on both the rotational frequency and the strength of the magnetic field in striking difference from the other mechanisms. We also show that gravitational waves can be produced by polar gap regions due to their rapid charge-discharge process that takes place in timescales from nanosec to microsec. This can provide an alternative way to probe magnetars and test the polar gap model.

Since the first detection of gravitational waves (GW) a few years ago [1], a lot of effort has been concentrated on this front both theoretically and experimentally. With the advent of Pulsar Timing Arrays and a series of new interferometers that have been proposed and expected to enter operation in the near or far future, there has been a lot of interest for new astrophysical GW sources that can potentially reveal a lot of information regarding astrophysical and cosmological processes. One field that has been studied extensively for obvious reasons is the production of GW by neutron stars (NS). Due to their compactness, there is a lot of opportunity to emit GW under certain conditions. NS can get involved in binaries among themselves or with black holes. This is the strongest type of signal that can come from a NS and this has already been detected [2]. Other possible cases of GW emission by NS is via several non-radial oscillations modes that can be excited in principle either by internal processes or by encounters with bypassing objects. A rotating NS is more oblate in the equator. This by itself cannot produce any GW, since the latter requires a time varying quadrupole (or higher) moment. Therefore in case for example a bypassing object disturbs the rotation of the NS, a nonzero second derivative of the quadrupole moment can be created, leading to emission of GW. For gravitational waves produced by pulsating NS, see e.g. [3].

However, there is another subtle mechanism where GW can be produced by NS involving neither some internal process nor a bypassing object. As it is well known since the 60's, a rotating NS with a magnetic field cannot be without the presence of a magnetosphere [4]. In case where the rotation and magnetic axes do not coincide, the co-rotating magnetosphere can create GW that in principle can be detected in future experiments. This scenario has been already studied in [5] and [6] where the GW produced by the magnetosphere were deduced. The focus of these two papers was on the detectability of these GW in upcoming interferometers. Continuous GW produced in the context of glitches has been considered in [7].

In this paper we verify that indeed GW produced by the magnetosphere of NS with strong magnetic fields are within reach in upcoming experiments. In addition we show that this is a source of continuous GW with a spectrum consisting of two frequencies, i.e., the frequency of the NS rotation f_0 and $2f_0$ with a very specific relative amplitude between the two. Furthermore we focus on another aspect of this scenario. We study how the emission of such GW by the magnetosphere affects the first and second braking index of the NS. We shall argue that in case of magnetars with extremely high magnetic fields, the braking index can be substantially over 3 which is the number expected in standard scenarios where the NS deceleration takes place due to magnetic dipole radiation and/or via torques of escaping to infinity currents from the poles of the NS. We find that unlike the usual magnetic dipole and aligned rotator models where the braking index is independent of both the rotation frequency and the magnetic field, in high magnetic field magnetars, the braking index depends on both mentioned quantities. Similar conclusions can be drawn for the second braking index. We will show that small deviations from the standard values result from NS with fields of at least 10^{16} Gauss and significant deviations are expected for fields of 10^{18} to 10^{20} Gauss. Although such extremely high magnetic fields have not been observed in magnetars so far, this is not unexpected. Arguments based on the virial theorem suggest fields up to 10^{18} Gauss for NS with nuclear cores [8], while for magnetars with a quark core this value can rise to 10^{20} Gauss [9]. Hybrid stars with quark and nuclear matter and high magnetic fields have been studied in [10]. The effects of extremely high magnetic fields on the QCD equation of state (relevant also for NS) has been recently readdressed [11, 12].

Finally we study an interesting effect within the framework of the polar gap model. The vacuum region above the polar cap discharges via sparks that create a cascade of positron-electron pairs that screen the electric field within a timescale that ranges from 10^{-9} to 10^{-5} sec. Within the volume of the polar gap, this quick discharge creates time varying fluctuations in the energy density

and quadrupole moment that produce GW with frequencies in the MHz-GHz range. Given the fact that the frequency range is much larger than that of the rotation, this effect albeit small in amplitude, could in principle provide a tool to test the polar gap model. It is worth mentioning that in this context, GW are emitted even if the rotation and magnetic axes are antiparallel.

GRAVITATIONAL WAVES PRODUCED BY THE MAGNETOSPHERE

As already mentioned the production of GW due to the co-rotating motion of the magnetosphere in the case where rotation and magnetic axes are not aligned has been studied in [5] and [6]. Here we repeat the calculation within the quadrupole approximation. This introduces a minor as it turns out error in the estimate of the GW compared e.g. to [6] where the calculation does not implement this approximation. However the quadrupole approximation allows us to provide results for any angle α between the rotation and magnetic axes and not just only for the case of $\alpha = \pi/2$. In addition we do not implement a slow rotation approximation ignoring higher powers of ωR (ω and R being the angular frequency and radius of the NS) as in [6].

We model the magnetic field of the star to be given by a typical magnetic dipole of the form

$$\vec{B} = \frac{3\hat{r}(\hat{r} \cdot \vec{m}) - \vec{m}}{r^3}, \quad (1)$$

where \vec{m} is the magnetic dipole with magnitude $B_0 R^3$ (B_0 being the magnetic field at the surface of the star). We assume that the magnetic axis subtends an angle α with the rotation axis and therefore $\vec{m} = B_0 R^3 (\sin \alpha \cos \omega t, \sin \alpha \sin \omega t, \cos \alpha)$. Upon the assumption that the NS is to a good approximation a perfect conductor, the presence of the magnetic dipole field in a rotating NS induces an electric field of the form

$$\vec{E} = -(\vec{\omega} \times \vec{r}) \times \vec{B}, \quad (2)$$

in order for the Lorentz force applied to every charged particle to be zero in the co-rotating frame. We use $c = 1$. As it was demonstrated in [4] in a rotating NS with a magnetic field, the induced electric field causes particles to detach from the star and fill up the surrounding space, thus creating a magnetosphere. The individual components of the electric field are

$$\begin{aligned} E_r &= -\frac{m\omega}{2r^2} (\sin \alpha \sin 2\theta \cos(\omega t - \phi) - 2 \cos \alpha \sin^2 \theta), \\ E_\theta &= -\frac{2m\omega}{r^2} \sin \theta (\sin \alpha \sin \theta \cos(\omega t - \phi) + \cos \alpha \cos \theta), \\ E_\phi &= 0. \end{aligned} \quad (3)$$

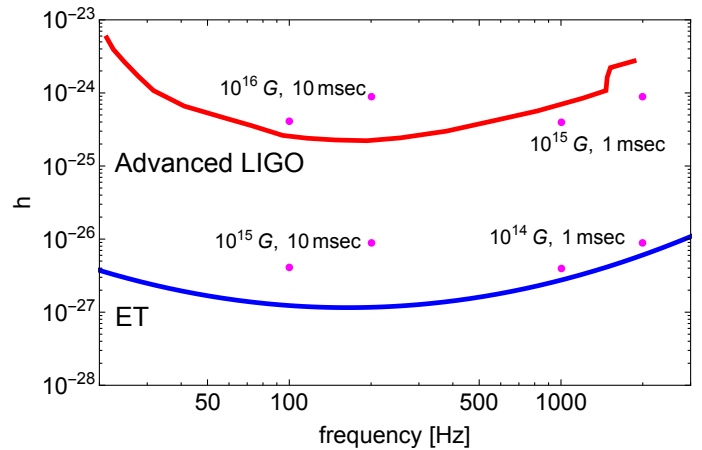


FIG. 1: GW amplitude produced by the magnetosphere for NS of various magnetic fields and rotation periods. We have chosen $\alpha = \psi = \pi/4$. Each choice appears as a doublet in the frequency domain, one with frequency that of the NS rotation f_0 and $2f_0$. Note that for $\alpha = \pi/2$ only the $2f_0$ component survives. The signal is calibrated with sources at a distance of 1 kpc.

The contribution to the energy density from the electric and magnetic fields is $\rho = (E^2 + B^2)/(8\pi)$ where the components of both fields can be read off by Eqs. (1) and (3). The quadrupole moment is

$$Q_{ij} = \int d^3x \rho(x, t) (x_i x_j - \frac{1}{3} \delta_{ij} r^2). \quad (4)$$

Since the magnetosphere co-rotates with the star, the integration is limited within the light cylinder i.e., at distances up to $\omega r \sin \theta = 1$. Given that the time dependence of the quadrupole moment enters in the time variation of the energy density, we can calculate both the amplitude of the GW and the energy emitted in that form:

$$h_{ij}^{TT} = \frac{2G}{r} \Lambda_{ij,kl} \ddot{Q}_{kl}(t - r), \quad (5)$$

where $\Lambda_{ij,kl}$ is the appropriate projection operator for the transverse traceless gauge. Using Eqs. (1) and (3) we can calculate the energy density and subsequently the the second derivative of the quadrupole moments by use of Eq. (4), getting

$$\begin{aligned} \ddot{Q}_{11} &= -\ddot{Q}_{22} = AB_0^2 R^5 \omega^2 \cos 2\omega t \sin^2 \alpha, \\ \ddot{Q}_{12} &= AB_0^2 R^5 \omega^2 \sin 2\omega t \sin^2 \alpha, \\ \ddot{Q}_{13} &= CB_0^2 R^5 \omega^2 \sin 2\alpha \cos \omega t, \\ \ddot{Q}_{23} &= CB_0^2 R^5 \omega^2 \sin 2\alpha \sin \omega t, \\ \ddot{Q}_{33} &= 0. \end{aligned} \quad (6)$$

The coefficients A and C are given by

$$\begin{aligned}
A &= -\frac{2}{5} - \frac{3\pi\omega R}{64} + \frac{10\omega^2 R^2}{21}, \\
C &= -\frac{1}{10} + \frac{2\omega^2 R^2}{35}.
\end{aligned}
\tag{7}$$

Note that in the case where $\alpha \neq \pi/2$ (and $\alpha \neq 0, \pi$), there are two frequencies emitted i.e., ω and 2ω , contrary to the case where $\alpha = \pi/2$ where only the 2ω is emitted. This is quite important in recognising and identifying such a signal. In the most probable scenario $\alpha \neq \pi/2$ and therefore it is of crucial importance for interferometers to not only detect the two frequencies but also the relative strength between the two. To this end, upon assuming that the detector lies in a direction forming an angle ψ with the rotational axis of the NS and having chosen conveniently a corresponding $\phi = 0$, we can estimate the two modes of GW [13]

$$\begin{aligned}
h_+ &= \frac{G}{r} (\ddot{Q}_{11} - \cos^2 \psi \ddot{Q}_{22} - \sin^2 \psi \ddot{Q}_{33} + \sin 2\psi \ddot{Q}_{23}) = \\
&= \frac{G}{r} B_0^2 R^5 \omega^2 [A(1 + \cos^2 \psi) \sin^2 \alpha \cos 2\omega t \\
&\quad + C \sin 2\psi \sin 2\alpha \sin \omega t], \\
h_\times &= \frac{2G}{r} (\cos \psi \ddot{Q}_{12} - \sin \psi \ddot{Q}_{13}) = \\
&= \frac{2G}{r} B_0^2 R^5 \omega^2 (A \cos \psi \sin^2 \alpha \sin 2\omega t - C \sin \psi \sin 2\alpha \cos \omega t).
\end{aligned}
\tag{8}$$

This signal makes a very concrete prediction. Apart from the characteristic signal of ω and 2ω frequencies, a system of interferometers could in principle determine the angle ψ . Consequently since A and C depend only on ω (which will be accurately determined) and R , the independent detection of the two modes h_+ and h_\times could also determine both the angle α and R (which in any case does not vary a lot for a NS). In principle such a signal can test our knowledge with respect to the NS magnetosphere and give us information regarding also the magnetic field. To get a sense of the strength of the GW, we can write the overall factor in the previous equation in appropriate units

$$\begin{aligned}
&\frac{G}{r} B_0^2 R^5 \omega^2 \simeq \\
&3 \times 10^{-24} \left(\frac{B_0}{10^{15} \text{Gauss}} \right)^2 \left(\frac{R}{12 \text{ km}} \right)^5 \left(\frac{\text{msec}}{P} \right)^2 \left(\frac{\text{kpc}}{r} \right),
\end{aligned}
\tag{9}$$

where P is the period of the rotation measured in milliseconds and r the distance to the NS in kiloparsecs. The amplitude of GW produced by the magnetosphere in the quadrupole approximation is depicted in Fig. 1 contrasted against the sensitivity of advanced LIGO and the Einstein Telescope. Since the signal produced in our studied context is not a burst but rather a continuous wave, we use the advanced LIGO O2 constraints on continuous waves [14], where three different methods have been implemented (i.e., FrequencyHough, SkyHough and

Time-Domain F-Statistics). Continuous waves are constrained more compared to bursts and inspirals since the observation time can be in principle as long as a year. Similarly we used the analysis for continuous waves for the Einstein Telescope data [15]. We converted the constraint on the ellipticity of NS to a constraint on the continuous GW amplitude which consequently turns out to be more accurate (due to the longer observation time) from constraints on inspirals and bursts. For fixed parameters i.e. magnetic field B and frequency of the NS rotation f_0 , the results depicted in Fig. 1 come in pairs of two monochromatic GW of frequencies f_0 and $2f_0$. One can see from the figure that e.g. $B = 10^{16}$ Gauss NS with periods of 10^{-3} sec can already be excluded within distances of kpc.

BRAKING INDEX

NS slow down effectively due to two main mechanisms i.e., via magnetic dipole radiation and the Goldreich-Julian mechanism of the aligned rotator [4]. In the first case, the fact that the axis of the magnetic field does not align with that of rotation, induces emission of electromagnetic waves via radiation of the precessing magnetic dipole. In the second case, currents of charged particles that are emitted from the caps of the NS in the presence of the magnetic field induce a torque that opposes the motion of the NS, thus acting as an impeding force for the motion of the star. In general GW can be emitted when there is a time varying quadrupole moment. Although the rotation itself changes the shape of the NS making it oblate, unless there are bumps on the surface of the star, such shape does not create GW because the quadrupole moment remains unchanged in time. However any misalignment between the principal axes of the NS and the rotation axis creates GW. An assessment of possible detection of continuous GW in this case for the Einstein Telescope has been given in [15].

However as it has been pointed out firstly in [5] and [6] and we argued in the previous section, the misalignment of the magnetic field with the rotation axis leads to emission of GW that also contribute to the rotational deceleration of the NS even in the absence of misalignment between principal and rotation axes.

Formally the energy loss of rotational kinetic energy due to emission of electromagnetic waves when both mechanisms are present is [16]

$$\frac{dE}{dt} = -L_{\text{mag}} \sin^2 \alpha - L_{\text{align}} \cos^2 \alpha,
\tag{10}$$

where the terms that appear in the right hand side correspond to the magnetic dipole and aligned rotator respectively and they are given by

$$L_{\text{mag}} = \frac{B_0^2 \omega^4 R^6}{4}, \quad L_{\text{align}} = \frac{B_0 \omega \omega_F R^3 I}{2},
\tag{11}$$

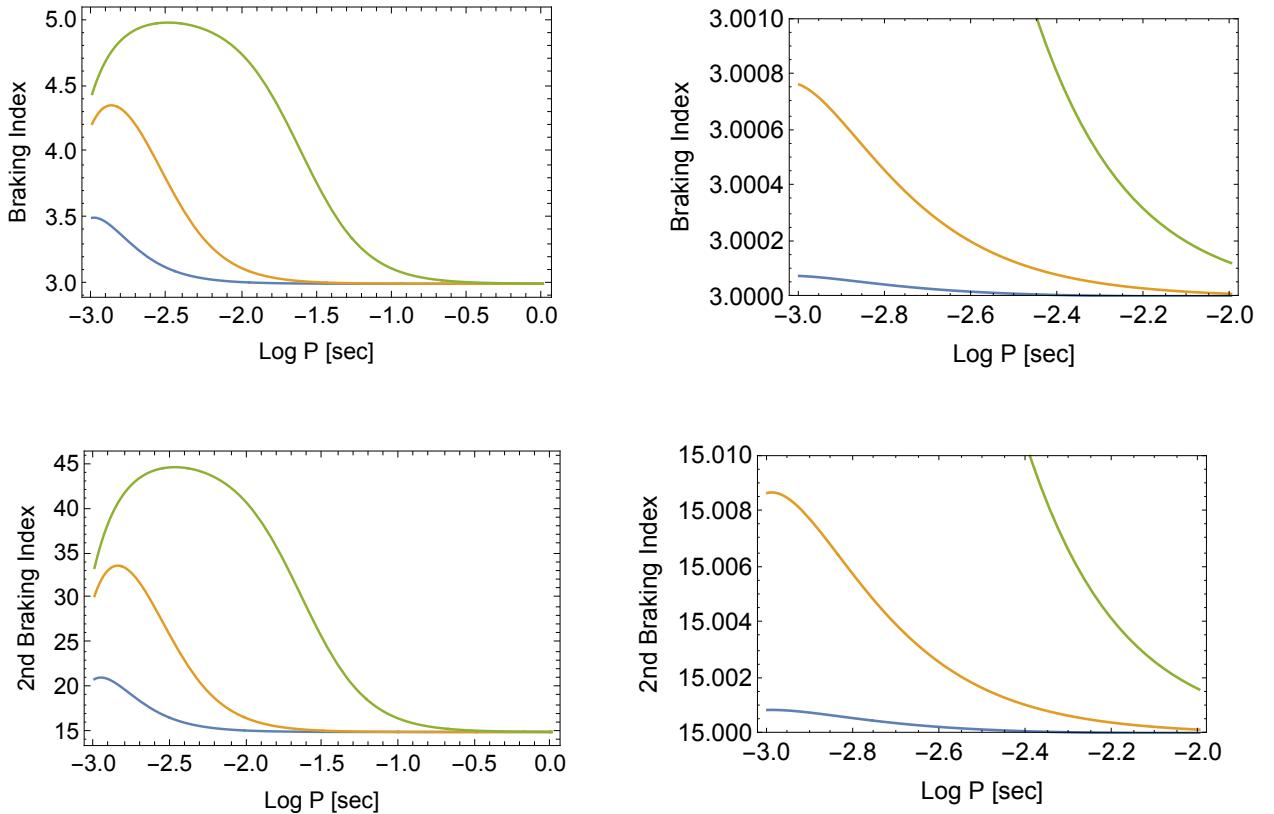


FIG. 2: First (upper panels) and second (lower panels) braking indices for magnetars of different magnetic field as a function of $\text{Log } P$ (P being the period of the star in sec). *Upper Left panel:* From higher index value to lower, we have stars with $B = 10^{20}$, 10^{19} and $10^{18.5}$ Gauss. *Right panel:* The same thing for $B = 10^{17.5}$, 10^{17} and $10^{16.5}$ Gauss. *Lower panels:* Same as the upper panels for the second braking index. In all plots we use $R = 20$ km and $\alpha = \pi/2$.

where $\omega_F = \omega - \omega_{\text{death}}$, (ω_{death} being the angular velocity where the pulsar stops emitting). The current I has been estimated in the seminal paper of Goldreich and Julian [4] indicating the charge current emitted by the polar caps. It is given by

$$I_{GJ} = \frac{B_0 R^3 \omega^2}{2}. \quad (12)$$

Combining the last three equations, taking into account the energy loss due to GW emission and provided that we are interested in angular velocities $\omega \gg \omega_{\text{death}}$, the overall energy loss reads

$$\frac{dE}{dt} = -\frac{B_0^2 \omega^4 R^6}{4} - GB_0^4 \omega^6 R^{10} f_E(\alpha, \omega R), \quad (13)$$

where f_E is an appropriate function of α and ωR . It can be estimated using the fact that the energy loss rate due to GW within the quadrupole approximation is given by

$$\frac{dE}{dt} = -\frac{G}{5} \langle \ddot{Q}_{ij} \ddot{Q}_{ij} \rangle, \quad (14)$$

where the brackets denote average over a period. The first term in the right hand side of Eq. (13) is the sum of

the two electromagnetic contributions. Note that since in the limit $\omega \gg \omega_{\text{death}}$ their contributions are equal, the α angle dependence drops out. The second term is the contribution coming from the emission of GW. The rate of energy loss is related to the angular velocity deceleration via $dE/dt = -I\omega\dot{\omega}$ where I is the moment of inertia of the rotating NS. The first and second braking indices are defined respectively as

$$n = \frac{\ddot{\omega}}{\dot{\omega}^2}, \quad m = \frac{\dot{\omega}\omega^2}{\dot{\omega}^3}. \quad (15)$$

Measuring the braking index for a NS is no easy task. It requires the estimate (apart from angular frequency ω itself) of the first and second derivative of ω . Therefore there is no surprise that the braking index has been determined only for a handful of NS (see e.g. [17, 18] and references therein). These measured braking indices are all below 3 and they have been determined with varying accuracy ranging from 0.001 to 0.1. The second braking index is even harder to measure [21]. It requires the estimate of the third derivative of ω which is known only for the Crab pulsar [19] and PSR B1509-58 [20].

For any mechanism where $\dot{\omega} = -k\omega^n$ with k independent of time, the braking index is n and the second braking index is $m = n(2n - 1)$. By inspection of Eq. (13) both the aligned rotator model and the magnetic dipole model give $n = 3$ and $m = 15$. Note also that GW emission provides first and second braking indices $n = 5$ and $m = 45$ respectively. The co-existence of the electromagnetic emission mechanisms with the GW emission one will make both n and m depart from their corresponding values of 3 and 15. This is depicted in Fig. (2) where both the first and second braking indices are plotted as a function of the rotational period. Pulsars with magnetic fields as low as $\sim 10^{16}$ Gauss could cause deviations from $n = 3$ starting from 10^{-4} . Such accuracy can be anticipated for some pulsars in the future given the current one which can be as low as 10^{-3} . However even larger magnetic fields of the order of 10^{18} Gauss can cause a significant change in both n and m as it can be seen. As expected, faster rotations cause in general larger deviations from the standard $n = 3$ and $m = 15$ values. Note however that this is not completely true when we look at potential pulsars with periods below 10 msec. As it can be seen in the figure, both n and m in this mechanism are not decreasing functions of the period within the whole range of parameters. Both indices increase in the msec range as the period increases reaching a maximum and after that indeed n and m become decreasing functions of the period. This is in distinct contrast to what happens to the braking index that is dominated by GW emission under the condition that the GW emission is due to misalignment between the principal axes and the rotation one, which is expected to have braking indices monotonically decreasing with the period. This feature is attributed to the nontrivial way that powers of ωR enter the expression of the quadrupole moment. It reflects the nontrivial way that the GW emission depends on the rotation and magnetic field. Ordinarily, higher frequency means larger GW amplitude. However in this case, higher frequency leads also to smaller light cylinder and thus smaller volume that contributes to the GW emission. Note here that for a large part of the studied parameter space, it appears that the deviation from the standard value of m is roughly an order of magnitude larger than that of n . This is anticipated and certainly true when the deviations are small. Another characteristic feature which is distinctly different from the typical GW emission due to the misalignment of an oblate principal axis with respect to the rotation axis or due to the existence of bumps in the surface of the star is the fact that in our studied scenario, both indices depend strongly on the magnetic field unlike the former cases. The magnetic field of NS is typically estimated by the deceleration rate of the rotation. However in principle, a different independent estimate of the magnetic field could actually test our scenario. In any case, even if the magnetic field cannot be determined independently, knowledge of both n and m can poten-

tially distinguish this deceleration mechanism from the standard one that is independent of the magnetic field since in our studied scenario both n and m depend on the magnetic field nontrivially. As a final comment it is worth looking at models of decaying magnetic field. In such a context the magnetic field can be correlated to the rotational frequency. This could provide another way to test this mechanism since it could make a concrete prediction on both indices once the correlation between the magnetic field and rotational frequency is established.

GRAVITATIONAL WAVES FROM THE POLAR CAP

Due to symmetry and reflected in Eq. (6), when the magnetic field is parallel or antiparallel to the rotation axis, there is no emission of GW. However even in this case there is a potential source for GW production at least within models that exhibit polar gaps. The aforementioned picture of Goldreich and Julian portrayed earlier where the rotation of the NS causes emission of particles from the poles is not accurate due to the inability of extraction of positive charges. As a result, polar gaps might form [22], which inside them there is no charge. This lack of the appropriate Goldreich-Julian charge density allows the development and growth of electric fields that are parallel to the magnetic dipole field. As time goes on, the electric field and the gap increase. It had been shown that the gap cannot increase indefinitely. In fact the maximum height that the gap can reach cannot exceed the size of the polar region with a radius r_p which is basically the radius of a disk centered with the magnetic and rotation axis where magnetic field lines departing from inside the disk cross the light cylinder. As it was argued in [22], under reasonable conditions, curvature photons that are produced by particles accelerated within the gap can lead to a spark that discharges the gap, i.e., a cascade of positron-electron pair production. The electric field accelerates positrons and electrons in opposite directions, thus discharging the gap. Ruderman and Sutherland argue that the discharge process takes place in timescales of microsec which is roughly the time it takes for a relativistic particle to travel across the polar gap multiplied by a factor ~ 40 . Once discharged and filled with the appropriate Goldreich-Julian charge density, the electric field drops to zero. The Goldreich-Julian current I_{GJ} quickly depletes once again the charge from the polar gap and the electric field starts growing again. This happens within a similar timescale since charges are flying off the region with the speed of light. This cycle of charging and discharging the polar cap region in short timescales with rapid changes of extremely high electric fields can potentially induce GW as mentioned earlier even in the case where the star has the magnetic dipole and rotation axis in an antiparallel fashion.

Estimating accurately the GW spectrum is complicated. As the gap grows in height and strength of the electric field, it gets the same time depleted by charge. These charged particles are dispersed in the space of the magnetosphere outside the polar gap. Therefore a precise determination of the GW signal would require two ingredients: i) knowledge of how charged particles are dispersed outside the polar gap as the latter is evacuated and ii) an accurate knowledge of the evolution of the electric field as a function of time and space. Here we make an approximate analysis for the amplitude of the GW produced based on a simplified toy model. Nevertheless, a lot of insight can be gained from such an attempt. On the one hand this studied effect produces GW even in the case where there is no misalignment between rotation and magnetic axes. On the other hand, due to the fact that the timescale involved in this process is not the period of the NS but the timescale of discharge which is considerably smaller, the GW frequency is of the order of at least 10^5 Hz. This is a signal at high frequencies, away from the frequency band of several GW astrophysical sources. To this end and for the sake of simplicity, for the estimate of the quadrupole moment that will drive the GW production we will consider only the variation of the electric field. The magnetic field is expected to stay constant and therefore does not source any GW in this scenario. Since we are interested in a ballpark estimate of the signal, we do not consider the complicated change of the density of the charged particles. This will hopefully introduce an error that can be of order one.

We adopt a simple model for the variation of the electric field similar to [23]. We assume that the electric field evolves linearly with time and that the gap grows also linearly in height with the speed of light up to a maximum height h . This is justified by the fact that the Goldreich-Julian current evacuates charges practically with the speed of light. This depletion of charge is what creates the electric field component parallel to the z -axis. Within our approximation the electric field is

$$E(z) = E_{\max} \frac{z - R}{h}, \quad (16)$$

where z denotes the coordinate along the rotation axis. Note that during the charging of the gap $t = z - R - T/2$ for $-T/2 \leq t \leq -T/2 + h$. T is the total period of the cycle charge-discharge that we will estimate later on. Within our approximation after the electric field reaches its maximum, it will stay there up to time $t = T/2 - h$ where the spark ignites. After that moment the charge redistributes and reaches the Goldreich-Julian value that screens completely the electric field. Therefore after $t = T/2 - h$ and until $T = T/2$, we have $t = T/2 + R - z$. Note also that z is measured from the center of mass which in good approximation is taken to be the center of the star. Fig. (3) illustrates the geometry of the polar cap region.

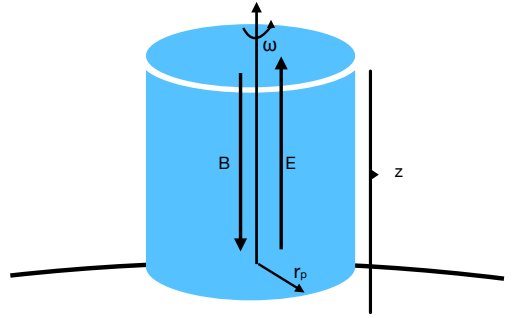


FIG. 3: The polar gap in the case of antiparallel magnetic field and rotational axis. The height of the gap grows linearly with time with the speed of light up to a maximum value h , upon which a spark discharges the gap reducing its height and electric field linearly with time until it gets zero.

Within our setup we can estimate the quadrupole moment of the polar gap. For example

$$M_{11} = \int \frac{1}{8\pi} E(z)^2 x^2 dx dy dz, \quad (17)$$

where the integration takes place within the cylinder of radius r_p and height z . Here $M_{ij} = \int d^3x \rho(x, t) x_i x_j$ is the quadrupole moment without the second term inside the integral of Eq. (4) that makes it traceless. Given the dependence on z of the electric field (see Eq. (16)), we have

$$\begin{aligned} M_{11} = M_{22} &\simeq \frac{E_{\max}^2 r_p^4}{96h^2} f(t) \\ M_{33} &\simeq \frac{E_{\max}^2 r_p^2 R^2}{24h^2} f(t), \end{aligned} \quad (18)$$

with

$$f(t) = \begin{cases} (t + \frac{T}{2})^3 & -\frac{T}{2} \leq t \leq -\frac{T}{2} + h \\ h^3 & -\frac{T}{2} + h \leq t \leq \frac{T}{2} - h \\ (\frac{T}{2} - t)^3 & \frac{T}{2} - h \leq t \leq \frac{T}{2} \end{cases}. \quad (19)$$

Since the function $f(t)$ is periodic, one can expand it in Fourier series of frequencies nf_0 where $f_0 = 1/T$. After that, the second time derivative can be taken in order to estimate the amplitude of the GW. However, it is not expected that the process of charge/discharge is strictly periodic. This deviation from strict periodicity will smooth out the spectrum. In addition one could only take the derived spectrum as a very rough estimate given the crudeness and the uncertainty of the approximation we used to model the whole charge-discharge cycle. In all the benchmark points we present (see Table I), we find that $T \gg h$. Although the fundamental frequency will be f_0 , by inspection of the function $f(t)$, it is understood

that the rapid changes which will induce the largest contribution to the GW production is rather $f_1 = 1/h$ which is much higher than f_0 . In fact the Fourier analysis verifies exactly this: the signal appears at f_0 but the amplitude peaks at f_1 . Higher frequencies than f_1 can also be unsuppressed. Due to the ambiguity regarding the precise form of $f(t)$ we will give an approximate estimate of the produced amplitude of GW as follows. Taking twice the time derivative of Eq. (18) yields

$$\begin{aligned}\ddot{M}_{11} = \ddot{M}_{22} &\simeq \frac{E_{\max}^2 r_p^4}{16 h} g(t) \\ \ddot{M}_{33} &\simeq \frac{E_{\max}^2 r_p^2 R^2}{4 h} g(t) \\ \ddot{M}_{12} = \ddot{M}_{13} = \ddot{M}_{23} &= 0,\end{aligned}\quad (20)$$

where in \ddot{M}_{33} we have omitted terms of the order of h/R and T/R . The function $g(t)$ within our approximation is given by

$$g(t) = \begin{cases} \frac{t+\frac{T}{2}}{h} & -\frac{T}{2} \leq t \leq -\frac{T}{2} + h \\ 0 & -\frac{T}{2} + h \leq t \leq \frac{T}{2} - h \\ \frac{\frac{T}{2}-t}{h} & \frac{T}{2} - h \leq t \leq \frac{T}{2} \end{cases} \quad (21)$$

By inspection of Eq. (20), for relatively slow rotations $\ddot{M}_{33} \gg \ddot{M}_{11}$ because $R \gg r_p \simeq R\sqrt{\omega R}$. To give an approximate estimate for the GW amplitude, we note that $g(t)$ is of order one for time between $-T/2 \leq t \leq -T/2 + h$ and $T/2 - h \leq t \leq T/2$. As we mentioned earlier the Fourier analysis gives a peak at $f_1 = h^{-1}$ and a smaller amplitude at $f_0 = T^{-1}$, consistent with our argument here.

In order to determine the ballpark frequencies f_0 and f_1 of the produced GW we need an estimate of h and T . In the standard picture of [22], a gap where the Goldreich-Julian charge density is absent develops, leading to the creation of a potential difference $\delta V = \omega B h^2$. A single particle accelerates within the gap producing a number of curvature photons which each of them in turn creates a pair of positron-electron. The mean free path for these curvature photons is exponentially sensitive to the magnetic field and the size of the gap h . Due to that, once the mean free path becomes $\sim h$ it will lead to an exponential production of pairs that will ignite the spark that will discharge the gap. This happens when [22]

$$h \simeq 5 \times 10^3 \rho_6^{2/7} P^{3/7} B_{12}^{-4/7} \text{ cm}, \quad (22)$$

where ρ_6 is the magnetic field curvature length measured in units of 10^6 cm, $B_{12} = B/(10^{12} \text{ Gauss})$ and P the period of the NS rotation in sec. The charged particles accelerate within the gap to energies

$$E_{\text{gap}} \simeq \omega B h^2 = 1.6 \times 10^{12} B_{12}^{-1/7} P^{-1/7} \rho_6^{4/7} \text{ eV}. \quad (23)$$

This energy leads to a relativistic factor $\gamma = E_{\text{gap}}/m_e$ where m_e is the mass of the electron. Each of these

B (Gauss)	ρ_6	f_0 (MHz)	f_1 (GHz)	h_+
10^{13}	1	3.2	0.4	1.4×10^{-32}
10^{14}	0.01	0.9	6	1.02×10^{-31}
10^{15}	1	11.1	2.2	2.7×10^{-29}
10^{16}	1	23.6	4.8	1.2×10^{-27}
10^{17}	1	50	10	5.8×10^{-26}

TABLE I: Benchmark points for different magnetic fields and curvature parameter ρ_6 . f_0 is the fundamental frequency given by the inverse timescale needed for the charge/discharge cycle T^{-1} and f_1 is the frequency corresponding to the rapid timescale h^{-1} where the signal becomes maximum (see text). h_+ is the strength of the GW. For all cases the rotation period of the NS has been taken to be 10^{-3} sec and the distance to the source 1 kpc.

charged positrons and electrons will create along their path inside the gap an average number of curvature photons

$$N_\gamma \simeq \frac{4}{9} e^2 \frac{h}{\rho} \gamma. \quad (24)$$

We can give now a rough estimate of the timescale needed to produce enough charge in the gap vacuum to discharge it. Within the timescale of h which is the time it takes for a particle to cross the gap, N_γ curvature photons are produced, which at time $2h$ each of them has produced one electron-positron pair. The amount of required charge in order to discharge the gap is given by the Goldreich-Julian density which over the poles is $\rho_e = -\vec{\omega} \cdot \vec{B} / (2\pi)$. Therefore the amount of charge needed is $|Q| = \rho_e \pi r_p^2 h$. Within this simple argument, the number of pairs grows as a geometrical series every $2h$, leading to $T \sim 2h \ln[(2N_\gamma - 1)Q / (2N_\gamma e)] / \ln(2N_\gamma)$. For example for a NS with $B_{12} = P = \rho_6 = 1$, we get $T \sim 24h$, while for $B_{12} = \rho_6 = 1$ and $P = 10^{-2}$, we get $T \sim 38$. These results are comparable to the range given in [22]. However we should stress that in order to discharge the gap, two conditions have to be fulfilled: i) the mean free path for converting the curvature photons to electron-positron pairs has to be smaller than h and ii) N_γ must be larger than 0.5 or more in order for the pair creation to grow at each time h . h cannot become larger than r_p and therefore as a NS slows down and ω decreases, the gap increases. When the gap becomes $h \sim r_p$, the pulsar ceases to emit because there can be no discharge and production of electron-positron pairs. We are interested in NS with large magnetic fields. As the magnetic field increases, Eq. (22) shows that h drops and subsequently N_γ drops too (see Eq. (24)). Therefore at some magnetic field, N_γ becomes smaller than 0.5 and there is no cascade of electron-positron pairs created. In this case it is expected that h will increase as much needed, as long as $h \leq r_p$, until N_γ becomes of order 1.

The h_+ and h_\times can be estimated by use of Eq. (8). Note that this equation holds also if we replace Q_{ij} with

M_{ij} . Because $\ddot{M}_{12} = \ddot{M}_{13} = 0$, we have $h_{\times} = 0$. Therefore a very characteristic feature of this emission mechanism (for $\alpha = \pi$) is the absence of h_{\times} modes. The h_{+} mode is given by

$$h_{+} = \frac{G}{r}(\ddot{M}_{11} - \ddot{M}_{33})\sin^2\psi. \quad (25)$$

As we mentioned $\ddot{M}_{11} \ll \ddot{M}_{33}$. Ignoring the factor $\sin^2\psi$ and setting the distance to the source to 1kpc, we can estimate the amplitude for different benchmark points presented in Table I. f_0 and f_1 are the two frequencies mentioned earlier. The amplitude for h_{+} that is presented refers to f_1 . Depending on the exact form of the functions $f(t)$ or $g(t)$, the amplitude at f_0 will be somewhat suppressed compared to that at f_1 that we quote at the table. For all benchmark points we used a period for the magnetar of 10^{-3} sec. Although for the moment there are no current experiments probing the MHz-GHz range of frequencies, several proposals for future experiments exist, aiming exactly at detection of high frequency GW [24]. Table 1 of [24] gives a summary of all the high GW frequency proposals. Among the different proposals, detectors based on enhanced magnetic conversion could in principle operate at ~ 10 GHz with a sensitivity for the strain 10^{-30} to 10^{-26} . Similarly for superconducting rings, the projected sensitivity at 10 GHz is 10^{-31} . By inspection of Table I magnetic fields as low as 10^{14} Gauss are above the threshold in the GHz frequency range of the aforementioned proposals.

We can now generalize the emission of GW for an angle that is not $\alpha = \pi$. If we call the coordinates we used in the problem which we studied above where the rotation axis is antiparallel to the magnetic field axis x'_i , we can relate them to the fixed space coordinates x_i where generically the magnetic field subtends an angle α with the rotation axis via $x'_i = R_{ij}x_j$, where $R = R_x(\pi - \alpha)R_z(\omega t)$ is a rotation transformation matrix which is the product of a rotation around x -axis by angle $\pi - \alpha$ times a rotation around z -axis by ωt (ω being the angular rotational frequency of the NS). The quadrupole tensor in the two coordinates systems is related via $Q = R^T Q' R$. Once the quadrupole tensor is known, one can estimate the GW spectrum in the generic case. There are two main observations regarding the generic case. The first one is that for $\alpha \neq \pi$, h_{\times} is no longer zero. The second one is that apart from the frequency $\Omega = 2\pi/T$ (which is related to the charge-discharge process), there are also the frequencies $\Omega \pm \omega$ and $\Omega \pm 2\omega$. In general $\Omega \gg \omega$ and therefore all frequencies lie close to each other. However the combination of all these frequencies makes a very characteristic signal which if and once the high frequency (MHz-GHz) range of GW is probed, it could facilitate the identification of this polar gap effect.

In this paper we studied the GW that can be induced by the magnetosphere of rapidly rotating magnetars. We found that this is within reach in upcoming detectors un-

der sensible assumptions. We also found that this GW emission can affect the first and second braking index of magnetars as long as the magnetic fields are strong. Finally we studied the effect of the charging and discharging in the polar gap model. This process can lead to production of GW with frequencies in the MHz and GHz range which currently is not probed by any experiment, although several future proposals and upcoming detectors are in play. The detection of such a signal will be able to test the polar gap models especially on magnetars.

Several directions can be taken in the future in order to improve our estimates. One in principle should attempt to include in the changing quadrupole moment of the polar gap, the incoming and outgoing plasma contribution which could change the amplitude of the GW signal by a factor of order one. This is not a priori an easy task since it would require probably some magnetohydrodynamics simulations of the plasma. Furthermore a more accurate description of the charge-discharge process should be implemented. This has been studied to some extent in [25–27]. For example sophisticated simulations of the process where curvature photons decay to electron-positron pairs which in turn accelerate within the polar gap and emit new curvature photons has been considered in [28]. An implementation of a more accurate time evolution of the electric field could significantly change the shape of the power spectrum of the emitted GW but it will not probably change significantly the main frequency f_1 and the amplitude of the GW. Nevertheless it can be crucial in identifying accurately the effect in future high frequency GW detectors.

-
- [1] B. P. Abbott *et al.* [LIGO Scientific and Virgo], Phys. Rev. Lett. **116**, no.6, 061102 (2016) doi:10.1103/PhysRevLett.116.061102 [arXiv:1602.03837 [gr-qc]].
 - [2] B. P. Abbott *et al.* [LIGO Scientific and Virgo], Phys. Rev. Lett. **119**, no.16, 161101 (2017) doi:10.1103/PhysRevLett.119.161101 [arXiv:1710.05832 [gr-qc]].
 - [3] N. Andersson and K. D. Kokkotas, Int. J. Mod. Phys. D **10**, 381-442 (2001) doi:10.1142/S0218271801001062 [arXiv:gr-qc/0010102 [gr-qc]].
 - [4] P. Goldreich and W. H. Julian, Astrophys. J. **157**, 869 (1969) doi:10.1086/150119
 - [5] E. Nazari and M. Roshan, Mon. Not. Roy. Astron. Soc. **498**, no.1, 110-127 (2020) doi:10.1093/mnras/staa2322 [arXiv:2001.05392 [astro-ph.HE]].
 - [6] I. Contopoulos, D. Kazanas and D. B. Papadopoulos, Mon. Not. Roy. Astron. Soc. **527**, no.4, 11198-11205 (2023) doi:10.1093/mnras/stad3913 [arXiv:2312.11586 [gr-qc]].
 - [7] G. Yim, Y. Gao, Y. Kang, L. Shao and R. Xu, Mon. Not. Roy. Astron. Soc. **527**, no.2, 2379-2392 (2023) doi:10.1093/mnras/stad3337 [arXiv:2308.01588 [astro-ph.HE]].

- [8] D. Lai and S. L. Shapiro *Astrophys. J.*, **383**, 745 (1991)
- [9] E. J. Ferrer, V. de la Incera, J. P. Keith, I. Portillo and P. L. Springsteen, *Phys. Rev. C* **82**, 065802 (2010) doi:10.1103/PhysRevC.82.065802 [arXiv:1009.3521 [hep-ph]].
- [10] H. Sotani and T. Tatsumi, *Mon. Not. Roy. Astron. Soc.* **447**, 3155 (2015) doi:10.1093/mnras/stu2677 [arXiv:1412.4610 [astro-ph.HE]].
- [11] E. S. Fraga, L. F. Palhares and T. E. Restrepo, *Phys. Rev. D* **108**, no.3, 034026 (2023) doi:10.1103/PhysRevD.108.034026 [arXiv:2303.12140 [hep-ph]].
- [12] E. S. Fraga, L. F. Palhares and T. E. Restrepo, *Phys. Rev. D* **109**, no.5, 5 (2024) doi:10.1103/PhysRevD.109.054033 [arXiv:2312.13952 [hep-ph]].
- [13] M. Maggiore, Oxford University Press, 2007, ISBN 978-0-19-171766-6, 978-0-19-852074-0 doi:10.1093/acprof:oso/9780198570745.001.0001
- [14] B. P. Abbott *et al.* [LIGO Scientific and Virgo], *Phys. Rev. D* **100**, no.2, 024004 (2019) doi:10.1103/PhysRevD.100.024004 [arXiv:1903.01901 [astro-ph.HE]].
- [15] M. Branchesi, M. Maggiore, D. Alonso, C. Badger, B. Banerjee, F. Beirnaert, E. Belgacem, S. Bhagwat, G. Boileau and S. Borhanian, *et al.* *JCAP* **07**, 068 (2023) doi:10.1088/1475-7516/2023/07/068 [arXiv:2303.15923 [gr-qc]].
- [16] I. Contopoulos and A. Spitkovsky, *Astrophys. J.* **643**, 1139-1145 (2006) doi:10.1086/501161 [arXiv:astro-ph/0512002 [astro-ph]].
- [17] C. M. Espinoza, A. Lyne, M. Kramer, R. N. Manchester and V. Kaspi, *Astrophys. J. Lett.* **741**, L13 (2011) doi:10.1088/2041-8205/741/1/L13 [arXiv:1109.2740 [astro-ph.HE]].
- [18] O. Hamil, J. R. Stone, M. Urbanec and G. Urbanová, *Phys. Rev. D* **91**, no.6, 063007 (2015) doi:10.1103/PhysRevD.91.063007 [arXiv:1608.01383 [astro-ph.HE]].
- [19] A. G. Lyne, R. S. Pritchard and F. G. Smith *Mon. Not. R. Astron. Soc.* **233**,667 (1988)
- [20] V. M. Kaspi, R. N. Manchester, B. Siegman S. Johnston and A. G. Lyne *Astrophys. J.* **422**, L83 (1994)
- [21] A. Parthasarathy, S. Johnston, R. M. Shannon, L. Lentati, M. Bailes, S. Dai, M. Kerr, R. N. Manchester, S. Osłowski and C. Sobey, *et al.* *Mon. Not. Roy. Astron. Soc.* **494**, no.2, 2012-2026 (2020) doi:10.1093/mnras/staa882 [arXiv:2003.13303 [astro-ph.HE]].
- [22] M. A. Ruderman and P. G. Sutherland, *Astrophys. J.* **196**, 51 (1975) doi:10.1086/153393
- [23] A. Prabhu, *Phys. Rev. D* **104**, no.5, 055038 (2021) doi:10.1103/PhysRevD.104.055038 [arXiv:2104.14569 [hep-ph]].
- [24] N. Aggarwal, O. D. Aguiar, A. Bauswein, G. Cella, S. Clesse, A. M. Cruise, V. Domcke, D. G. Figueroa, A. Geraci and M. Goryachev, *et al.* *Living Rev. Rel.* **24**, no.1, 4 (2021) doi:10.1007/s41114-021-00032-5 [arXiv:2011.12414 [gr-qc]].
- [25] A. N. Timokhin, *Mon. Not. Roy. Astron. Soc.* **408**, 2092-2114 (2010) doi:10.1111/j.1365-2966.2010.17286.x [arXiv:1006.2384 [astro-ph.HE]].
- [26] A. N. Timokhin and J. Arons, *Mon. Not. Roy. Astron. Soc.* **429**, 20 (2013) doi:10.1093/mnras/sts298 [arXiv:1206.5819 [astro-ph.HE]].
- [27] E. A. Tolman, A. A. Philippov and A. N. Timokhin, *Astrophys. J. Lett.* **933**, no.2, L37 (2022) doi:10.3847/2041-8213/ac7c71 [arXiv:2202.01303 [astro-ph.HE]].
- [28] D. Noordhuis, A. Prabhu, S. J. Witte, A. Y. Chen, F. Cruz and C. Weniger, *Phys. Rev. Lett.* **131**, no.11, 111004 (2023) doi:10.1103/PhysRevLett.131.111004 [arXiv:2209.09917 [hep-ph]].